Editorial

We only see what we know: Structures at risk during the anterior intrapelvic approach

The classification, radiographic analysis, and surgical treatment of acetabular fractures described by Judet and Letournel in the 1960's laid the groundwork for current management of these difficult injuries [1]. The ilioinguinal approach, described in 1963, was the first intrapelvic approach that allowed for visualization of the medial wall of the acetabulum [2]. While this approach served as the workhorse for anterior open reduction of acetabular fractures, dissection through the inguinal canal is technically demanding, with mobilization of the iliac vessels and lymphatic system, risking thrombosis and lymphedema, respectively [3]. The Stoppa approach was first described for repair of inguinal hernias via an anterior midline incision that served as the basis for alternative approaches to intrapelvic fixation of acetabular fractures [4]. In the early 1990's Cole and Hirvensalo both described a modified Stoppa approach in which dissection was carried posteriorly and inferiorly [3] The modified Stoppa approach allows for visualization of the sciatic buttress, posterior column, quadrilateral surface, and anterior acetabulum.

Advances in plating technology, as well as surgical technique, have improved management of these challenging fractures. Traditionally fixed with pelvic reconstruction plates, newer quadrilateral surface buttress plates allow spanning of both columns and easier application through the modified Stoppa approach [5–8]. While the various surgical steps for this surgical exposure are well known, a thorough description of anatomical structures at risks encountered during dissection, especially postero-medially, is lacking. Evaluation of the anatomy specific to the AIP approach is essential so as to help acetabular surgeons avoid iatrogenic injuries.

We therefore conducted a study on five fresh frozen cadavers (3 men, 2 women) with a mean age of 58 years (range 49–72). The study protocol was approved by the local Institutional Ethical Committee Board.

Angiography

Each specimen was placed in the supine position on a radiolucent operating table. Intraperitoneal dissection through a vertical midline dissection was performed and the infra-renal descending aorta was ligated. One hundred milliliters of green silicone with radiopaque barium sulfate was injected into the common iliac artery on both sides and left to harden.

Internal fixation

Radiopaque 3D-printed models of the Stryker PRO Quadrilateral Surface infrapectineal and suprapectineal plates were fabricated to prevent artifact with computed tomography (CT). The infrapectineal plate was placed on the left acetabulum by aligning the posterior aspect of the plate parallel to the posterior border of the quadrilateral surface and fixed anteriorly at the superior pubic rami. The suprapectineal plate was fixed to the right acetabulum using the same technique. The obturator artery and nerve consistently crossed over the medial surface of the quadrilateral surface plate, as they were dissected and released to insert the plate beneath them [Fig. 1].

The intersection between pelvic brim and anterior SI joint was marked with a 3.5 mm titanium screw. This point, easily identified during surgery, served as a Reference Point (RP) from which the distances to at-risk structures were measured during dissection and on CT scan.

Cadaveric measurement

A lower abdominal vertical midline incision was made to remove the colon. Starting proximally, the common iliac artery, internal iliac artery (IIA) and vein (IIV), external iliac artery (EIA) and vein (EIV), superior gluteal artery (SGA), inferior gluteal artery (IGA), and sciatic nerve (SN) were dissected. The closest distance between these structures to both the plate and to the RP was measured using a digital caliper. Two authors separately analyzed and measured the closest distance between the plate and RP to the structure and recorded the average of the two measurements.

CT measurement

An axial CT scan of the pelvis with 1 mm slices and 3D reconstruction (Siemen1, Somatom definition) was performed [Fig. 2]. The CT cuts were standardized by aligning the anterior superior iliac spines and pubis in the coronal plane for accurate measurement. The common iliac artery was traced distally to identify the EIA, the IIA, the anterior division of IIA (and obturator artery branch), and posterior division of IIA (with SGA, inferior gluteal artery, and internal pudendal artery branches). The closest distance from the plate and the RP to the IIA, SGA, and EIA were measured in mm.
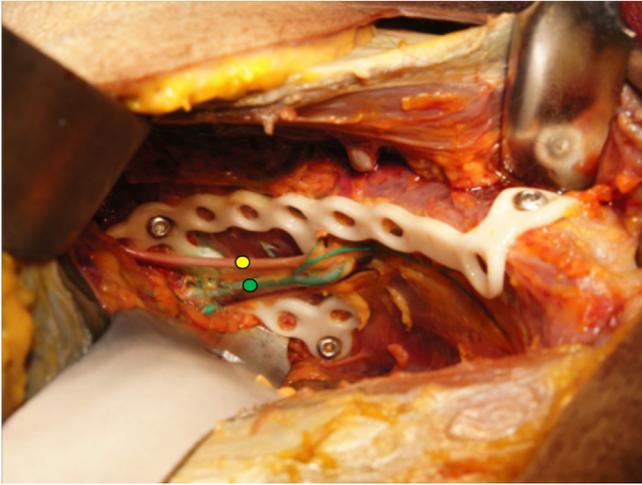
Fig. 1. Obturator nerve (yellow dot) and artery (green dot) crossing the infrapectineal plate. (For interpretation of the references to colour in this figure legend, the reader is referred to the web version of this article.)

Results

Corona mortis

Of the five cadaveric specimens, three had bilateral corona mortis anastomoses. One cadaver had a unilateral corona mortis, and one cadaver had none. The distance from the pubic symphysis to the corona mortis ranged from 3.6 to 7.2 cm. On all specimens the corona mortis anastomosed the obturator and external iliac arteries [Fig. 3].

Superior gluteal artery

Upon dissection, there was variation in the location where the SGA branched from the IIA. With a more proximal branch point, the SGA is closer to the plate and RP than the IIA. With a more distal branch point, the IIA has closer proximity to the plate and RP [Fig. 4]. On average, the SGA was observed on both dissection and CT to travel in closer proximity to infrapectineal plating site compared to the suprapectineal plate (Table 1).

Internal iliac artery

Similar to the SGA, the IIA was found on average to travel in closer proximity to the posterior extension of the infrapectineal plate on both dissection and CT scan observation. There was variation in the distance between the IIA and the RP based on laterality (Table 2).

Internal iliac vein

On the right hemipelvis, the closest structure to the suprapectineal plate and reference point is the internal iliac vein, which lies in proximity to the inferior aspect of the SI joint [Fig. 5] (Table 3).
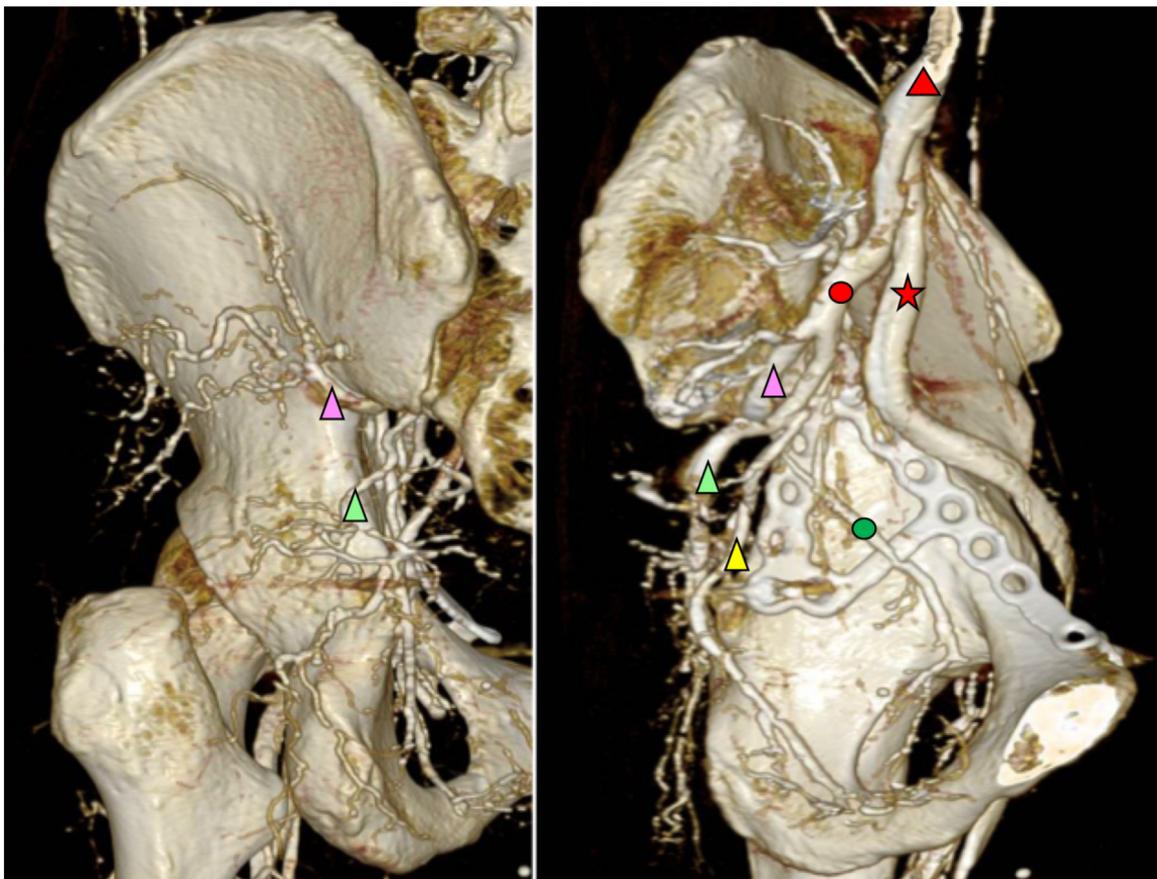

Fig. 2. 3D Reconstruction of a pelvic CT Angiogram identifying the common iliac artery (red triangle), EIA (red star), IIA (red circle), SGA (pink triangle), inferior gluteal artery (green triangle), internal pudendal artery (yellow triangle), and obturator nerve (green circle). (For interpretation of the references to colour in this figure legend, the reader is referred to the web version of this article.)
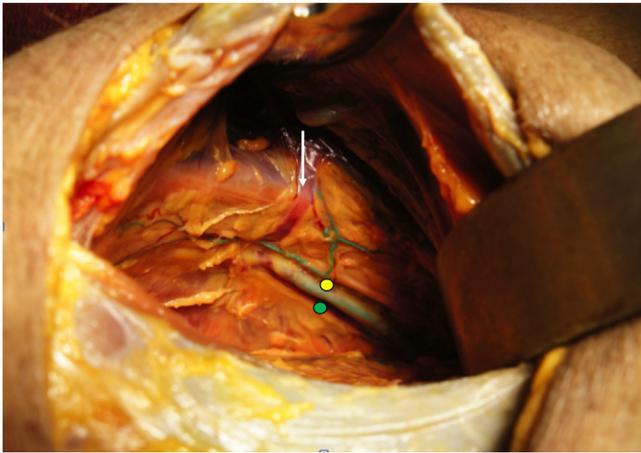
Fig. 3. Corona mortis (white arrow) visualized anastomosing with obturator artery (green circle). Yellow circle: obturator nerve. (For interpretation of the references to colour in this figure legend, the reader is referred to the web version of this article.)
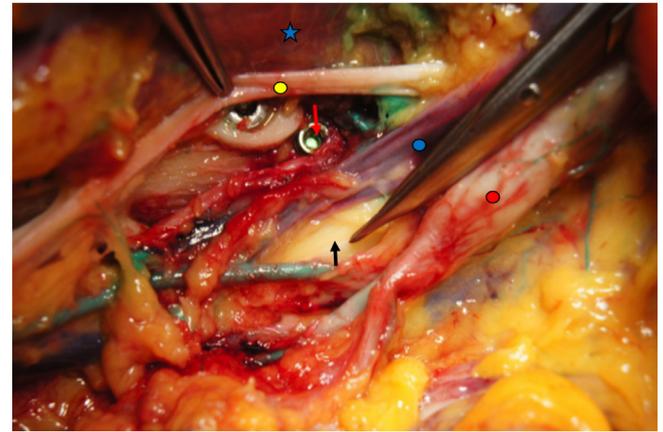

Fig. 4. SGA (pink triangle) visualized branching from IIA (red circle) near the proximal aspect of the suprapectineal plate. Also identified: Common iliac artery (red triangle), EIA (red star), Common iliac vein (blue triangle), EIV (blue star), IIV (blue circle), obturator nerve (yellow circle) and artery (green circle). (For interpretation of the references to colour in this figure legend, the reader is referred to the web version of this article.)

Table 1
Distance from superior gluteal artery to plate and reference point.

	Distance from Plate		Distance from Reference Point	
	Left	Right	Left	Right
Mean Measurement by CT (range)	8.9 mm (1.7–14.5)	16.4 mm (13.2–17.0)	11.8 mm (6.1–15.5)	16.2 mm (8.9–24.4)
Mean Measurement by Dissection (range)	10.8 mm (6.0–14.4)	15.8 mm (9.3–19.4)	9.7 mm (8.5–10.9)	11.1 mm (6.4–16.8)

Table 2
Distance from internal iliac artery to plate and reference point.

	Distance from Plate		Distance from Reference Point	
	Left	Right	Left	Right
Mean Measurement by CT (range)	12.5 mm (7.3–21.2)	21.0 mm (16.0–25.1)	18.4 mm (13.3–25.0)	21.3 mm (18.4–25.6)
Mean Measurement by Dissection (range)	12.2 mm (6.2–19.4)	16.1 mm (14.3–18.5)	11.1 mm (2.3–13.1)	14.7 mm (13.1–17.1)

Fig. 5. The IIV (blue circle) is the closest structure to the suprapectineal plate and reference point (red arrow). The sciatic nerve (black arrow), IIA (red circle), EIV (blue star), and obturator nerve (yellow circle) are also identified. (For interpretation of the references to colour in this figure legend, the reader is referred to the web version of this article.)

Table 3
Distance from internal iliac vein to plate and reference point.

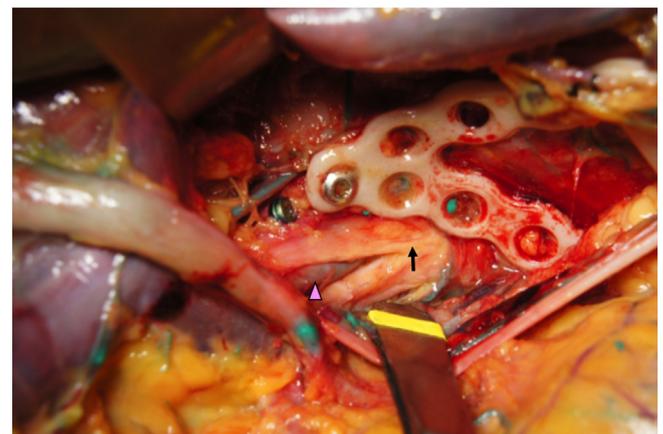|	Distance from Plate		Distance from Reference Point	
	Left	Right	Left	Right
Mean Measurement by Dissection (range)	14.8 mm (11.9–16.5)	7.6 mm (5.3–12.2)	12.4 mm (7.7–17.8)	3.7 mm (2.2–5.6)

Fig. 6. SGA (pink triangle) splitting the tibial and peroneal divisions of the sciatic nerve (black arrow). (For interpretation of the references to colour in this figure legend, the reader is referred to the web version of this article.)

Sciatic nerve

The sciatic nerve runs just medial to the reference point prior to passing through the sciatic notch. Some specimens showed the SGA passing between the tibial and peroneal divisions of the sciatic nerve [Fig. 6]. On the left side, the distance from the plate to the sciatic nerve ranged from 2.4 to 5.6 mm (mean 4.4 mm) and on the right side ranged 6.2–8.9 mm (mean 7.6 mm).

Discussion

Surgical fixation of acetabular fractures remains technically demanding due to the difficulty in gaining adequate exposure to

achieve safe anatomical reduction. The value of the AIP approach for reduction and fixation of acetabular fractures is well described [3,9,10]. Sagi et al. have demonstrated that excellent reduction of acetabular fractures is feasible through this approach. In a series of 57 patients, 59% had excellent reduction, 27% good reduction, and 14% poor reduction. Observed complications from the modified Stoppa approach included injury to the superior gluteal artery in one patient, one postoperative wound infection, and two direct inguinal hernias. Interestingly, one quarter of patients developed an obturator nerve palsy, attributed to excessive retraction or entrapment in fracture fragments [11].

With placement of infrapectineal plates, the internal iliac and superior gluteal arteries lie closest to the plate. The level at which the SGA branches determines its course past the plate, and with more proximal branch points the SGA will be the closest structure. In order to reduce and appropriately buttress the quadrilateral surface, the obturator nerve and artery must be identified and protected. The obturator nerve crosses the lower part of the SI joint, the pelvic brim, and lies close to the quadrilateral surface into the obturator foramen, while the obturator artery branches out from the anterior division of the IIA below the pelvic brim and below the obturator nerve into the obturator foramen. Cole et al. and Sagi et al. have both observed obturator nerve palsy from acetabular fixation through the modified Stoppa approach, and excessive retraction must be avoided [3,11]. Conversely, the internal iliac vein is the structure most at risk with placement of suprapectineal plates, which lie partially above the pelvic brim. As the IIV crosses over the pelvic brim, it lies just posterior to the suprapectineal plate. Application of the retractor medial to the SI joint at the pelvic brim should be avoid since the IIV is in close proximity to the SI joint.

The distance of the external iliac artery and external iliac vein to the RP and plate were not measured, as these structures are retracted during the exposure. However, careful placement of the second and third retractors is imperative to avoid damaging these structures.

Multiple factors led to variability in the observed measurements between specimens and between dissection and CT measurements. There was observed variation within specimens RP in relation to structures based on laterality and anatomic asymmetry. The relationship between structures with SGA and IIA depended greatly on the point of SGA branching. Additionally, the distance between the plate and measured structures varied based on specimen size. Measurement from the RP proved less prone to variability with change in specimen size. CT measurements varied from physical measurements as visualization of neurovascular structures is limited with dissection, and CT allows better evaluation of deeper structures.

The AIP approach allows for excellent visualization of intrapelvic anatomy, accurate reduction of complex fractures, and stable fixation of a majority of acetabular fractures. A thorough understanding of at-risk structures during the approach and plate placement is imperative to minimize complications while in close proximity to vital neurovascular structures. Our findings allows for a better understanding of intrapelvic danger zones with plate placement. Clinical application of these results will allow for safe, efficient acetabular surgery and optimize patient outcomes.

Source of funding

Declaration of Competing Interest

The rest of the authors have nothing to disclose.

References

[1] Judet R, Judet J, Letournel E. Fractures of the acetabulum: classification and surgical approaches for open reduction. Preliminary report. J Bone Joint Surg Am 1964;46:1615–46.

[2] Letournel E. The treatment of acetabular fractures through the ilioinguinal approach. Clin Orthop Relat Res 1993;(292):62–76.

[3] Cole JD, Bolhofner BR. Acetabular fracture fixation via a modified Stoppa limited intrapelvic approach. Description of operative technique and preliminary treatment results. Clin Orthop Relat Res 1994;(305):112–23.

[4] Stoppa RE, Rives JL, Warlaumont CR, Palot JP, Verhaeghe PJ, Delattre JF. The use of dacron in the repair of hernias of the groin. Surg Clin North Am 1984;64(2):269–85.

[5] ElNahal WA, Abdel Karim M, Khaled SA, Abdelazeem AH, Abdelazeem H. Quadrilateral plate fractures of the acetabulum: proposition for a novel classification system. Injury 2018;49(2):296–301, doi:http://dx.doi.org/10.1016/j.injury.2017.11.041.

[6] Qureshi AA, Archdeacon MT, Jenkins MA, Infante A, DiPasquale T, Bolhofner BR. Infrapectineal plating for acetabular fractures: a technical adjunct to internal fixation. J Orthop Trauma 2004;18(3):175–8, doi:http://dx.doi.org/10.1097/00005131-200403000-00009.

[7] Yang Y, Yi M, Zou C, Yan Z, Yan X, Fang Y. Mapping of 238 quadrilateral plate fractures with three-dimensional computed tomography. Injury 2018;49(7):1307–12, doi:http://dx.doi.org/10.1016/j.injury.2018.05.026.

[8] Tanoğlu O, Alemdaroğlu KB, İltar S, Özmeriç A, Demir T, Erbay FK. Biomechanical comparison of three different fixation techniques for anterior column posterior hemitransverse acetabular fractures using anterior intrapelvic approach. Injury 2018;49(8):1513–9, doi:http://dx.doi.org/10.1016/j.injury.2018.06.020.

[9] Verbeek DO, van der List JP, Tissue CM, Helfet DL. Long-term patient reported outcomes following acetabular fracture fixation. Injury 2018;49(6):1131–6, doi:http://dx.doi.org/10.1016/j.injury.2018.04.031.

[10] Verbeek DO, Ponsen KJ, van Heijl M, Goslings JC. Modified stoppa approach for operative treatment of acetabular fractures: 10-year experience and mid-term follow-up. Injury 2018;49(6):1137–40, doi:http://dx.doi.org/10.1016/j.injury.2018.03.031.

[11] Sagi HC, Afsari A, Dziadosz D. The anterior intra-pelvic (modified rives-stoppa) approach for fixation of acetabular fractures. J Orthop Trauma 2010;24(5):263–70, doi:http://dx.doi.org/10.1097/BOT.0b013e3181dd0b84.

Theerachai Apivatthakakul[a,b]
aDepartment of Orthopaedics, Faculty of Medicine, Chiang Mai University, Thailand

bResearch cluster in Osteology Research and Training Center, Chiang Mai University, Thailand

Michael Maher
Allison Tetreault
Department of Orthopaedics, Denver Health Medical Center, Denver, CO, United States

Thanawat Buranaphatthana
Department of Orthopaedics, Faculty of Medicine, Chiang Mai University, Thailand

Sutiwat Luangsod
Department of Orthopaedics, Faculty of Medicine, Chiang Mai University, Thailand

Motasem Salameh
Joshua A. Parry
Cyril Mauffrey[*]
Department of Orthopaedics, Denver Health Medical Center, Denver, CO, United States

* Corresponding author at: Department of Orthopaedics, Director of Orthopaedic Trauma, Denver Health Medical Center, 777 Bannock Street, 80204 Denver, CO, United States.
E-mail address: Cyril.mauffrey@dhha.org (C. Mauffrey).